

Collective Properties of Low-lying Octupole Excitations in $^{208}_{82}Pb_{126}$, $^{60}_{20}Ca_{40}$ and $^{28}_8O_{20}$

X.R. Zhou^{a,b}, E.G. Zhao^{a,b,d}, B.G. Dong^c, X.Z. Zhang^c,
G.L. Long^{a,d}

^a*Department of Physics, Tsinghua University, Beijing 100084, P.R. China*

^b*Institute of Theoretical Physics, Chinese Academy of Sciences, Beijing 100080, P.R. China*

^c*China Institute of Atomic Energy, P.O. Box 275, Beijing 102431, P.R. China*

^d*Center of Theoretical Physics, National Laboratory of Heavy Ion Accelerator, Lanzhou 730000, P.R. China*

Abstract

The octupole strengths of β -stable nucleus $^{208}_{82}Pb_{126}$, a neutron skin nucleus $^{60}_{20}Ca_{40}$ and a neutron drip line nucleus $^{28}_8O_{20}$ are studied by using the self-consistent Hartree-Fock calculation plus the random phase approximation (RPA) with Skyrme interaction. The collective properties of low-lying excitations are analyzed by using particle-vibration coupling. The results show that the lowest isoscalar states above threshold in $^{60}_{20}Ca_{40}$ and $^{28}_8O_{20}$ are the superpositions of collective excitations and unperturbed transitions from bound state to nonresonance states. For these three nuclei, both the low-lying isoscalar states and giant isoscalar resonance carry isovector strength. The ratio $B(IV)/B(IS)$ is checked. It is found that, for $^{208}_{82}Pb_{126}$, the ratios are equal to $(\frac{N-Z}{A})^2$ in good accuracy, while for $^{60}_{20}Ca_{40}$ and $^{28}_8O_{20}$, the ratios are much larger than $(\frac{N-Z}{A})^2$. This results from the excess neutrons with small binding energies in $^{60}_{20}Ca_{40}$ and $^{28}_8O_{20}$.

PACS: 21.10.Re, 21.60.Ev, 21.60.Jz, 27.30.+t

Keywords: Neutron drip line nuclei; Collective excitations; Particle-vibration coupling; transition current; transition density

1 Introduction

Various new exotic properties are expected for nuclei far from β -stability. The collective properties of neutron drip line are especially interesting, because neutrons with small binding energies show a unique response to external fields.

In the Ref. [1–7], monopole, dipole and quadrupole isoscalar (IS) and isovector (IV) giant resonance in stable and drip line, particularly neutron drip line nuclei, were studied by using self-consistent Hartree-Fock (HF) plus random phase approximation (RPA) with Skyrme interaction, and the IS and IV correlation was taken into account simultaneously. It was found that for both β -stable and drip line nuclei the giant resonances can be well described by collective model [8,9]. For neutron drip line nuclei, however, there is appreciable amount of low-lying strengths just above threshold and these low-lying strengths are nearly pure neutron unperturbed excitations. For example, in Ref[4], quadrupole strength of the neutron drip line nucleus $^{28}_8O_{20}$ was analyzed and it was pointed out[4] that there exists so-called threshold strength, which is not of collective character and comes from the excitations of excess neutrons with small binding energies. For octupole excitations of nuclei, there are low-lying ($\Delta N = 1$) and high-lying ($\Delta N = 3$) excitations. In a recent publication [11], low-lying octupole excitation of a neutron skin nucleus $^{60}_{20}Ca_{40}$ was studied and it was pointed out the low-lying ($\Delta N = 1$) IS octupole states appear as collective excitations and are shifted down to very low energy region, which results from the disappearance of the magic number $N=50$. The low-lying octupole excitations usually consist of transitions from occupied states to bound states, resonance states and nonresonance states. Therefore, the collective properties of low-lying octupole excitation deserve to be studied for the further understanding. In this paper, we make more detailed study of low-lying ($\Delta N = 1$) octupole excitations of β -stable nucleus $^{208}_{82}Pb_{126}$, a neutron skin nucleus $^{60}_{20}Ca_{40}$ and a drip line nucleus $^{28}_8O_{20}$. It can be seen that in all these nuclei, the low-lying octupole states below and above threshold appear as collective excitations and the superpositions of collective and unperturbed excitations, respectively. The properties of these low-lying states can be understood from the point of view of particle-vibration coupling.

This paper is organized as follows. The theoretical formulism of HF plus RPA calculation is described in section 2. Numerical results and discussions are shown in section 3. A summary and conclusions are given in section 4.

2 formulism

The unperturbed strength function is defined by[12]

$$S_0 \equiv \sum_i |\langle i | Q^\lambda | 0 \rangle|^2 \delta(E - E_i) \\ = \frac{1}{\pi} \text{Im} \text{ Tr}(Q^{\lambda\dagger} G_0(E) Q^\lambda) \quad (1)$$

while RPA strength function is given by

$$\begin{aligned}
S &\equiv \sum_n |\langle n | Q^\lambda | 0 \rangle|^2 \delta(E - E_n) \\
&= \frac{1}{\pi} \text{Im} \text{Tr}(Q^{\lambda\dagger} G_{RPA}(E) Q^\lambda),
\end{aligned} \tag{2}$$

where G_0 is the noninteracting p-h Green function, and $G_{RPA}(E)$ is the RPA response function including the effect of the coupling to the continuum,

$$G_{RPA} = G_0 + G_0 v_{ph} G_{RPA} = (1 - G_0 v_{ph})^{-1} G_0. \tag{3}$$

In Eqs. (1) and (2), Q^λ expresses one-body operators, which are written as

$$Q_\mu^{\lambda=3,\tau=0} = \sum_i r_i^3 Y_{3\mu}(\hat{r}_i) \quad \text{for isoscalar octupole strength} \tag{4}$$

$$Q_\mu^{\lambda=3,\tau=1} = \sum_i \tau_z(i) r_i^3 Y_{3\mu}(\hat{r}_i) \quad \text{for isovector octupole strength} \tag{5}$$

The transition density for an excited state $|n\rangle$ is defined by

$$\delta\rho_{n0}(\vec{r}) \equiv \langle n | \sum_i \delta(\vec{r} - \vec{r}_i) | 0 \rangle, \tag{6}$$

which can be obtained by RPA response function

$$\delta\rho_{n0}(\vec{r}) = \alpha \int \text{Im}[G_{RPA}(\vec{r}, \vec{r}'; E_{res})] Q^\lambda(\vec{r}') d\vec{r}', \tag{7}$$

where the normalization factor α is determined from the transition strength $S(\lambda)$ as

$$\alpha = \frac{1}{\pi \sqrt{S(\lambda)}}. \tag{8}$$

The radial transition density is defined by

$$\delta\rho_{n0}(\vec{r}) \equiv \delta\rho_\lambda(r) Y_{\lambda\mu}^*(\hat{r}). \tag{9}$$

The transition current is evaluated as

$$J_{n0}(\vec{r}) = \langle n | \sum_i \frac{\hbar}{2mi} \{ \delta(\vec{r} - \vec{r}_i) \vec{\nabla}_i - \vec{\nabla}_i \delta(\vec{r} - \vec{r}_i) \} | 0 \rangle, \tag{10}$$

which can be expanded in the complete set of the vector spherical harmonics $\overrightarrow{Y}_{\lambda l, \mu}^*(\hat{r})$,

$$J_{n0}(\vec{r}) = (-i) \sum_{l=\lambda \pm 1} J_{\lambda l} \overrightarrow{Y}_{\lambda l, \mu}^*(\hat{r}), \quad (11)$$

where the radial current components $J_{\lambda l}$ are defined as

$$\begin{aligned} J_{\lambda l} &= i \int \overrightarrow{Y}_{\lambda l, \mu}(\hat{r}) J_{n0}(r) d\hat{r} \\ &= \langle n | \sum_i \frac{\hbar}{2m} \{ \delta(r - r_i) [Y_l^*(\hat{r}_i) \times (\vec{\nabla}_i^+ - \vec{\nabla}_i^+)]_{\lambda \mu} \} | 0 \rangle. \end{aligned} \quad (12)$$

The Bohr-Tassie model gives the transition density [8,9]

$$\delta \rho_{\lambda \tau}(r) \propto r^{\lambda-1} \frac{d \rho_0(r)}{dr} \quad \text{for } \lambda > 0 \quad (13)$$

and the radial current components [13]

$$J_{\lambda l} \propto \begin{cases} r^{\lambda-1} \rho_0(r) & \text{for } l = \lambda - 1 \\ 0 & \text{for } l = \lambda + 1. \end{cases} \quad (14)$$

In the present work, the properties of low-lying octupole excitations are studied from particle-vibration coupling. For octupole, we use the radial dependence of the particle-vibration coupling as

$$V_{\text{pv}}(r) \sim r^2 \frac{dU(r)}{dr} \quad (15)$$

or

$$V_{\text{pv}}(r) \sim r^2 \frac{d \rho_0}{dr}, \quad (16)$$

where $U(r)$ is the HF potential and $\rho_0(r)$ is the ground state density. Eq.(15) has been successfully used for the coupling of particle to shape oscillations [8].

The sign of the ratio

$$\frac{\langle p | V_{\text{pv}}(r) | h \rangle}{\langle p | r^3 | h \rangle} = \frac{\int \delta \rho_{ph}(r) V_{\text{pv}}(r) r^2 dr}{\int \delta \rho_{ph}(r) r^5 dr} \quad (17)$$

determines whether the particle-vibration coupling increases or decreases the strength of the unperturbed ph excitations[14]. The magnitude of the ratio is a measure that how strongly the unperturbed strength of this ph excitation is affected by performing RPA calculation. If the ratio is equal to zero, the unperturbed strength of this ph transition will remain unchanged by taking into account the RPA correlation.

3 Results and discussions

We first perform the HF calculation with the SkM interaction and then use the RPA with the same interaction including simultaneously both the IS and the IV correlation, which is solved in the coordinate space with the Green's function method, taking into account the continuum exactly.

The calculated unperturbed strengths of $^{208}_{82}Pb_{126}$, $^{60}_{20}Ca_{40}$ and $^{28}_8O_{20}$ are shown in Fig. 1. In harmonic oscillator model, the low-lying octupole strength ($\Delta N = 1$) is approximately equal to the high-lying ($\Delta N = 3$) strength in very large N limit, so the low-lying and high-lying octupole strength approximately exhausts 25% and 75% of the energy weighted sum rule, respectively. In real β -stable nuclei the N is finite, the low-lying strength is less than the value predicted by harmonic oscillator model in the large N limit. From Fig.1(a) it can be seen that for $^{208}_{82}Pb_{126}$, the unperturbed low-lying ($\Delta N = 1$) strength is centered at about 8 MeV and spread over the same order of energy range. It exhausts approximately 40% of total strength. The high-lying ($\Delta N = 3$) strength is centered at about 24 MeV and exhausts approximately 60% of total strength. For $^{60}_{20}Ca_{40}$, the unperturbed strength (see Fig.1(b)) is approximately spread over an energy range from 2 MeV to 15 MeV and exhausts about 60% of total strength. While for $^{28}_8O_{20}$ (see Fig.1(c)), except for a few high-lying proton excitations, nearly all of the octupole strength lies within the low energy region. For $^{60}_{20}Ca_{40}$ and $^{28}_8O_{20}$, large amount of neutron unperturbed octupole strengths are shifted down to very low energy region. This downward shifting of the octupole strengths is attributed to the disappearance of magic number $N=50$ for $^{60}_{20}Ca_{40}$ (see Fig.2(a)), and the disappearance of magic numbers $N=20$ and $N=28$ for $^{28}_8O_{20}$ (see Fig.2(b)). For all of these three nuclei, the calculated energy weighted sum rules are equal to the classical sum rules in a good accuracy.

In Fig.2, one-particle energies are given with a fixed neutron number for (a) $N=20$ and (b) $N=40$ as a function of proton number. It is easy to see that in Fig.2(a), when it is near the neutron drip line, the magic number $N=20$ is disappearing, which agrees with the experimental observation[15], and new magic number $N=16$ appears, which is consistent with the conclusion in Ref.[16]. The similar phenomena can be seen in Fig.2(b). When it is near the neutron drip

line, N=50 magic number is disappearing.

Fig .3 gives the IS and IV RPA octupole strength for $^{208}_{82}Pb_{126}$, $^{60}_{20}Ca_{40}$ and $^{28}_8O_{20}$. For β -stable nucleus $^{208}_{82}Pb_{126}$ (Fig.3(a)), we see an strong IS peak (below threshold) at Ex=3.48 MeV with strength $B(\lambda = 3, IS : 3^- \rightarrow 0^+) = 5.68 \times 10^5 fm^6$, which corresponds to $B(E3 : 3^- \rightarrow 0^+) = (\frac{Ze}{A})^2 \times 5.68 \times 10^5 fm^6 = 0.89 \times 10^5 e^2 fm^6$. These values are comparable to experimental values Ex=2.61 MeV and $B(E3 : 3^- \rightarrow 0^+) = 1.0 \times 10^5 e^2 fm^6$. The IS giant resonance is at about 20.5 MeV and the IV giant resonances are mainly distributed within the energy region from 25 MeV to 35 MeV.

For $^{208}_{82}Pb_{126}$, in Fig.4 and Fig.5 we show the transition densities and radial current components of IS excitation at Ex=3.48 MeV, IS giant resonance at Ex=20.5 MeV, and IV giant resonance at Ex=34.2 MeV, together with the prediction of Bohr-Tassie model. We see from these figures that these IS and IV octupole excitations are surface modes and the IS and IV giant resonances can be well described by collective model. For the strong collective IS state at Ex=3.48 MeV, in the central region of the nucleus there are some differences between two models, but in the surface region this excitation can well be described by Bohr-Tassie model.

In nuclei with neutron excess, the IS mode (shape vibration) gives rise to a IV moment which are proportional to (N-Z), so the strength of an IS mode carries IV strength, and the ratio of IV strength/IS strength is expected to be $(\frac{N-Z}{A})^2$ [4,10]. We calculated this ratio for collective IS modes at Ex=3.48 MeV and giant IS resonance around Ex=20.5 MeV in $^{208}_{82}Pb_{126}$. Both of these IS modes give the ratios which are equal to $(\frac{126-82}{208})^2$ in good accuracy.

For $^{60}_{20}Ca_{40}$ (Fig.3(b)), main IS strengths are shifted down to low energy region. Below 5 MeV there are 4 strong IS peaks and one of them is below threshold (Ex=1.91 MeV). From the transition densities and radial current components in Fig.6, it is seen that IS collective state at Ex=1.91 MeV can be described by Bohr-Tassie model. We are now to study the collectivity of the other three IS peaks below 5 MeV. The transition densities and radial current components for these three peaks are shown in Fig.7 and Fig.8, respectively. From Fig.7 it can be seen that these three IS peaks are surface modes and both neutrons and protons make contributions, which means they are collective. In the central region of the nucleus there are some differences between the transition densities of Bohr-Tassie model and those of RPA calculation, but in the surface region the results of RPA calculation are similar to those of collective model. From Fig.8 we see that for the currents the prediction of Bohr-Tassie model can hardly describe the RPA results, even in the surface region. For example, in our RPA calculation the small component $j_{3,4}(r)$ is comparable with the large component $j_{3,2}(r)$, but the Bohr-Tassie model should give $j_{3,4}(r) = 0$. This disagreement will be explained from the viewpoint of particle-vibration

coupling in the following of this paper.

The ratios of IV strength/IS strength for these 4 strong IS peaks (below 5 MeV) in $^{60}_{20}Ca_{40}$ are also calculated. We find that, however, unlike the case in β -stable nucleus $^{208}_{82}Pb_{126}$, the calculated ratios are larger than $(\frac{N-Z}{A})^2$ by factor 2 to 4 in $^{60}_{20}Ca_{40}$. This result is closely related to the neutron orbits with small binding energies and they make the unperturbed octupole strengths of transitions from these orbits appear in very low energy region.

For $^{28}_8O_{20}$ (see Fig.3(c)), the high-lying IS giant resonance nearly disappears and almost all the IS octupole strengths are shifted down to low energy region. We are now interested in the collective properties of the lowest three IS peaks in $^{28}_8O_{20}$. The transition densities and radial current components for these three peaks are shown in Fig.9 and Fig.10, respectively. From Fig.9 we see that these three peaks are surface modes and both protons and neutrons make contributions, and in Fig.1 and Fig.3 we notice that the IS strengths of these peaks are larger than unperturbed ones. That means they are collective. The Bohr-Tassie model can approximately describe the transition densities in the surface region of the nucleus. Fig.10 shows that the results of Bohr-Tassie model can hardly describe the currents properties of these IS peaks. The reason will be analyzed from the viewpoint of particle-vibration coupling in the following of this paper.

We also calculated the ratios of IV strength/IS strength for these three lowest IS peaks. The calculated values are factor 3 to 5 larger than the value of $(\frac{N-Z}{A})^2$ in $^{28}_8O_{20}$. Similar to $^{60}_{20}Ca_{40}$, this is also related to the small binding energies of the least bound neutrons.

Next we try to understand the collective properties of these low-lying IS excitations in $^{60}_{20}Ca_{40}$ and $^{28}_8O_{20}$ based on the particle-vibration coupling. We have checked that the signs of the ratio Eq. (17) in our cases are always positive, so we only consider their absolute values here. Fig.11 shows a few low-lying neutron unperturbed octupole strengths in $^{60}_{20}Ca_{40}$ for radial operators r^3 , $r^2 \frac{dU(r)}{dr}$ and $r^2 \frac{d\rho_0(r)}{dr}$, and Fig.?? shows the corresponding quantities for $^{28}_8O_{20}$, where $U(r)$ is the neutron radial HF potential and $\rho_0(r)$ is the ground state density. From Fig.11 we see that for the transition from bound state to nonresonance state $1f_{\frac{5}{2}} \rightarrow 3s_{\frac{1}{2}}$, there is a pronounced peak in octupole strength function for radial operator r^3 , but the corresponding peaks nearly disappear for the other two radial operators $r^2 \frac{dU(r)}{dr}$ and $r^2 \frac{d\rho_0(r)}{dr}$. For the transitions from bound states to resonance states $1f_{\frac{5}{2}} \rightarrow 2d_{\frac{5}{2}}$ and $2p_{\frac{1}{2}} \rightarrow 2d_{\frac{5}{2}}$, much like the transitions from bound states to bound states $1f_{\frac{5}{2}} \rightarrow 1g_{\frac{9}{2}}$ and $2p_{\frac{3}{2}} \rightarrow 1g_{\frac{9}{2}}$, there are strong peaks of octupole strengths for all of these three radial operators in corresponding energy region. It means that the ratios Eq. (17) for transitions to nonresonance states are much smaller than those for the transitions to resonance states and for the transitions to bound states, so when we perform RPA

calculation the unperturbed octupole strength of the radial operator r^3 for the transition from bound state to nonresonance state $1f_{\frac{5}{2}} \rightarrow 3s_{\frac{1}{2}}$ will be nearly unaffected, but the strengths of the radial operator r^3 for the transitions from bound states to resonance states and for the transitions from bound states to bound states will be strongly absorbed into collective excitations. Because the unperturbed octupole strength of the transition from bound state to nonresonance state $1f_{\frac{5}{2}} \rightarrow 3s_{\frac{1}{2}}$ for radial operator r^3 is mainly distributed within the energy region from 3.0 MeV to 4.5 MeV, so these three lowest IS peaks are the superpositions of unperturbed transition $1f_{\frac{5}{2}} \rightarrow 3s_{\frac{1}{2}}$ and collective excitations. That is why the collective model can not well describe the results of our RPA calculation, even in the surface region of the nucleus.

From Fig.12 we see similar results for $^{28}_8O_{20}$. For transition from bound state to nonresonance state $1d_{\frac{3}{2}} \rightarrow 2p_{\frac{3}{2}}$, the ratio Eq. (17) is much smaller than transitions from bound states to resonance states $1d_{3/2} \rightarrow 1f_{7/2}$ and $2s_{1/2} \rightarrow 1f_{7/2}$. The three lowest IS peaks are the superpositions of unperturbed transition $1d_{\frac{3}{2}} \rightarrow 2p_{\frac{3}{2}}$ and collective excitations. That is the reason why collective model can not well describe the results of our RPA calculation.

4 Summary and Conclusions

The octupole vibrations of β -stable nucleus $^{208}_{82}Pb_{126}$, a neutron skin nucleus $^{60}_{20}Ca_{40}$ and a drip line nucleus $^{28}_8O_{20}$ are studied and it is found that the lowest IS excitation below threshold for nuclei $^{208}_{82}Pb_{126}$ and $^{60}_{20}Ca_{40}$, and IS and IV giant resonances of β -stable nucleus $^{208}_{82}Pb_{126}$ can be well described by collective model, at least in the surface region.

For neutron skin nucleus $^{60}_{20}Ca_{40}$ and neutron drip line nucleus $^{28}_8O_{20}$, in the low-lying unperturbed neutron octupole strength ($\Delta N = 1$), there exist strengths of transitions from bound states to bound states, resonance states, and nonresonance states. The strengths of transitions to nonresonance states are nearly unaffected and the strengths of other transitions are strongly absorbed into collective states by taking into account the RPA correlation. So these lowest IS states above threshold are the superpositions of collective excitations and unperturbed transitions from bound states to nonresonance states.

We also find that, for β -stable nucleus $^{208}_{82}Pb_{126}$, both low-lying IS states and giant IS resonances carry IV component and the ratios of IV strength/IS strength are equal to $(\frac{N-Z}{A})^2$ in good accuracy, but for neutron skin nucleus $^{60}_{20}Ca_{40}$ and neutron drip line nucleus $^{28}_8O_{20}$, these ratios for a few lowest strong IS excitations are much larger than the values of $(\frac{N-Z}{A})^2$. These results are closely related to the small binding energies of neutron orbits in these nuclei. The octupole transitions from these orbits are mainly distributed in low en-

ergy region, so the contribution to low-lying ($\Delta N = 1$) octupole states from neutrons are much larger than those from protons.

This work is supported by the National Natural Science Foundation of China under contact 10047001 and the Major State Basic Research Development Program under contract No. G200077400. We are grateful to I. Hamamoto and H. Sagawa for providing us with continuum RPA program.

References

- [1] I. Hamamoto, H. Sagawa and X. Z. Zhang, Phys. Rev. C 53 (1996) 765.
- [2] I. Hamamoto and H. Sagawa, Phys. Rev. C 53 (1996) R1492.
- [3] I. Hamamoto and H. Sagawa, Phys. Rev. C 54 (1996) 2369.
- [4] I. Hamamoto, H. Sagawa and X. Z. Zhang, Phys. Rev. C 55 (1997) 2361; J. Phys. G 24 (1998) 1417.
- [5] I. Hamamoto, H. Sagawa and X. Z. Zhang, Nucl. Phys. A 626 (1997) 669.
- [6] I. Hamamoto, H. Sagawa and X. Z. Zhang, Phys. Rev. C 56 (1997) 3121.
- [7] I. Hamamoto, H. Sagawa and X. Z. Zhang, Phys. Rev. C 57 (1998) R1064.
- [8] A. Bohr and B. R. Mottelson, Nuclear Structure, Vol. II (Benjamin, New York, 1975).
- [9] L. T. Tassie, Australian, J. Phys. 9 (1956) 407.
- [10] F. Catara, E. G. Lanza, M. A. Nagarajan, and A. Vitturi, Nucl. Phys. A 614 (1997) 86.
- [11] I. Hamamoto, H. Sagawa and X. Z. Zhang, Phys. Rev. C 64 (2001) 024313.
- [12] I. Hamamoto, H. Sagawa and X. Z. Zhang, Nucl. Phys. A 648 (1999) 203.
- [13] T. Suzuki and D. J. Rowe, Nucl. Phys. A 286 (1977) 307.
- [14] I. Hamamoto nad X. Z. Zhang, Phys. Rev. C 58 (1998) 3388.
- [15] D. Guillemaud-Mueller, *et al.*, Nucl. Phys. A 426 (1984) 37; T. Motobayashi, *et al.*, Phys. Lett. B 346 (1995) 9.
- [16] A. Ozawa, T. Kobayashi, Y. Suzuki, K. Yashida and I. Tanihata, Phys. Rev. Lett. 84 (2000) 5439.

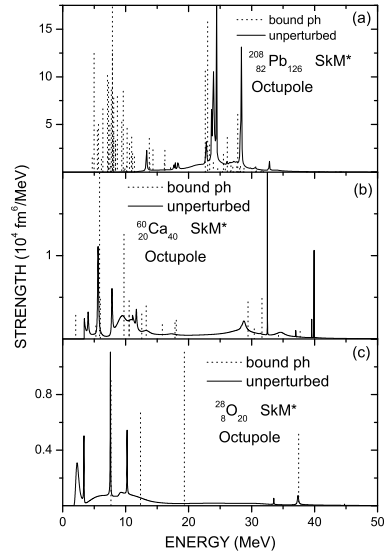


Fig. 1. Unperturbed octupole strengths of (a) $^{208}_{82}Pb_{126}$, (b) $^{60}_{20}Ca_{40}$ and (c) $^{28}_8O_{20}$.

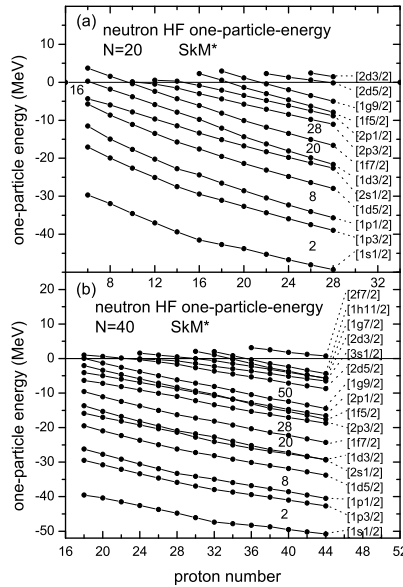


Fig. 2. One-particle energies vary with proton number for (a) neutron number $N = 20$ and (b) neutron number $N = 40$.

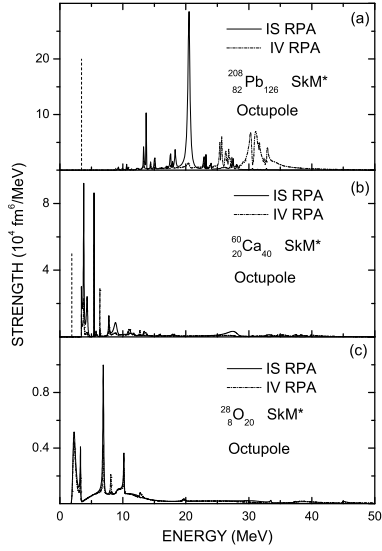


Fig. 3. Isoscalar and isovector octupole strengths of (a) $^{208}_{82}\text{Pb}_{126}$, (b) $^{60}_{20}\text{Ca}_{40}$ and (c) $^{28}_8\text{O}_{20}$.

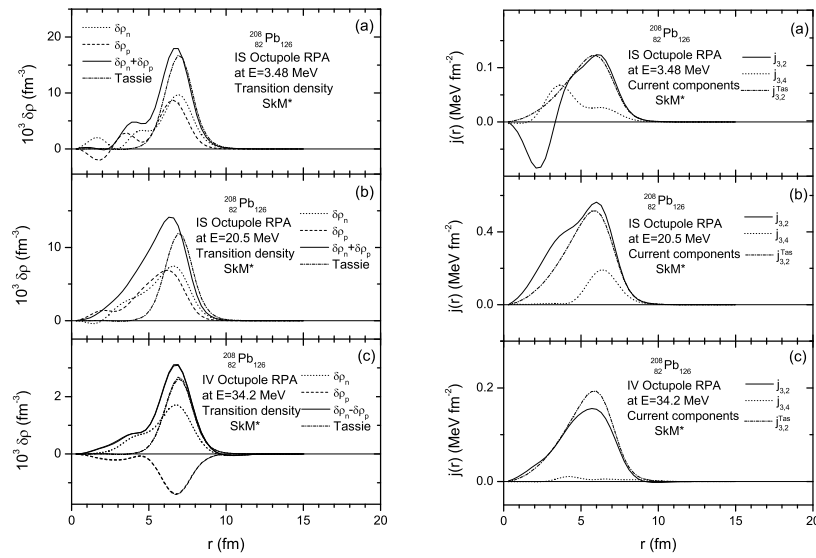


Fig. 4. (left) Radial transition densities of low-lying and high-lying IS and IV octupole modes of $^{208}_{82}\text{Pb}_{126}$.

Fig. 5. (right) Radial transition current components of low-lying and high-lying IS and IV octupole modes of $^{208}_{82}\text{Pb}_{126}$.

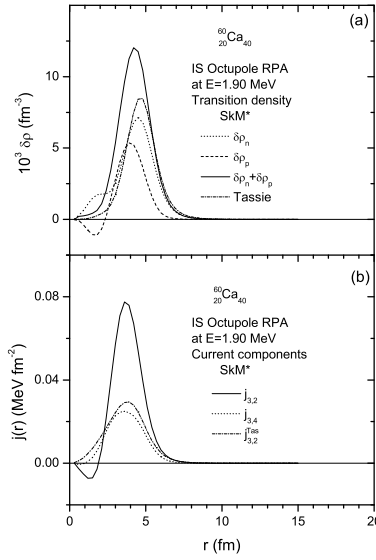


Fig. 6. Radial transition densities and current components of low-lying IS octupole modes of $^{60}_{20}Ca_{40}$.

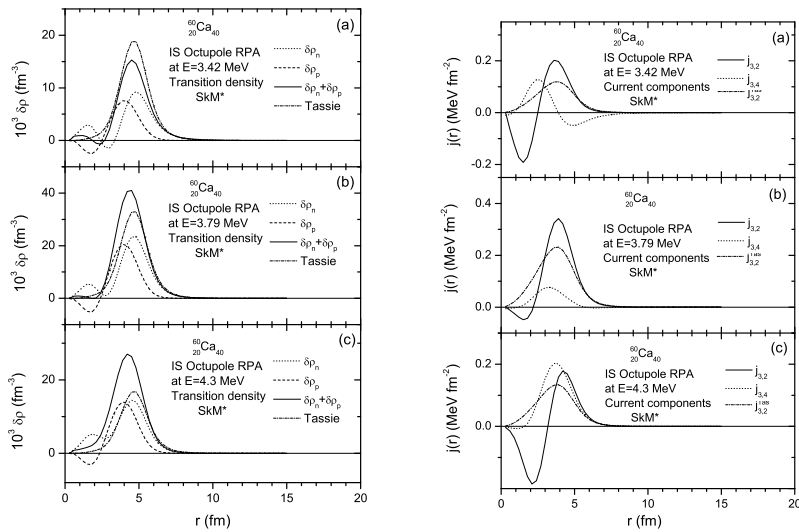


Fig. 7. (left) Radial transition densities of low-lying IS octupole modes of $^{60}_{20}Ca_{40}$.

Fig. 8. (right) Radial current components of low-lying IS octupole modes of $^{60}_{20}Ca_{40}$.

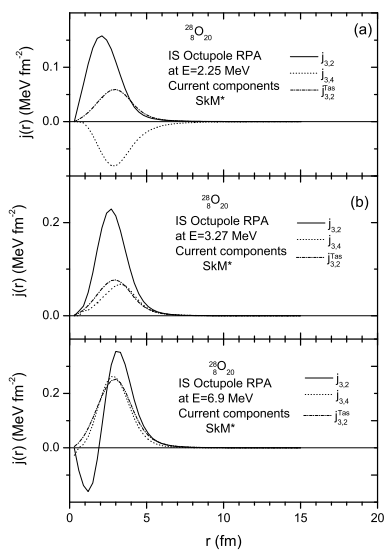
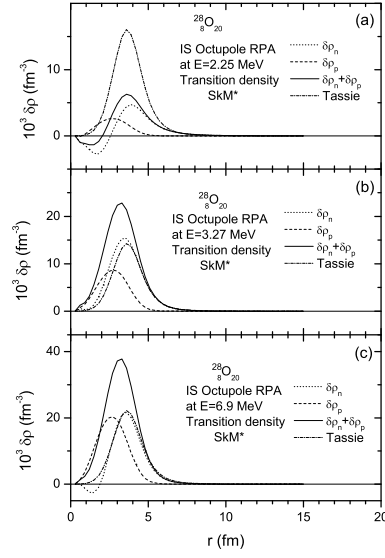


Fig. 9. (left) Radial transition densities of low-lying IS octupole modes of $^{28}_8O_{20}$.

Fig. 10. (right) Radial current components of low-lying IS octupole modes of $^{28}_8O_{20}$.

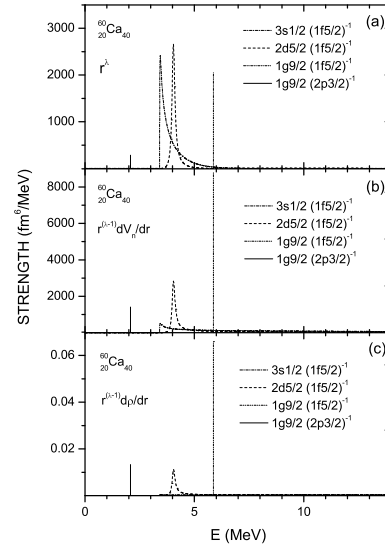


Fig. 11. Few low-lying unperturbed octupole strength in $^{60}_{20}Ca_{40}$ for radial operators (a) r^3 , (b) $r^2 \frac{dU(r)}{dr}$ and (c) $r^2 \frac{d\rho_0(r)}{dr}$, where $U(r)$ is the neutron radial HF potential and $\rho_0(r)$ is the ground state density.

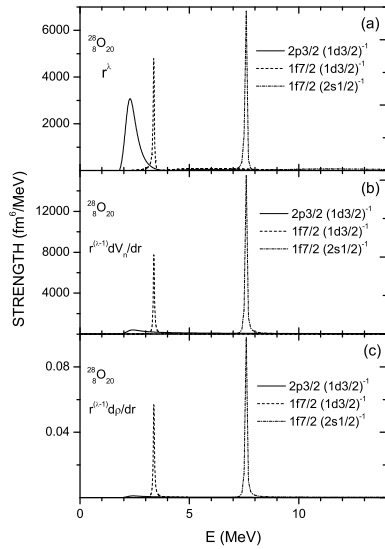


Fig. 12. Few low-lying unperturbed octupole strength in $^{28}\text{O}_{20}$ for radial operators (a) r^3 , (b) $r^2 \frac{dU(r)}{dr}$ and (c) $r^2 \frac{d\rho_0(r)}{dr}$, where $U(r)$ is the neutron radial HF potential and $\rho_0(r)$ is the ground state density.